Since January 2020 Elsevier has created a COVID-19 resource centre with free information in English and Mandarin on the novel coronavirus COVID-19. The COVID-19 resource centre is hosted on Elsevier Connect, the company's public news and information website.

doi:10.1016/j.jmb.2007.11.081 J. Mol. Biol. (2008) 376, 23–34

JMB

Available online at www.sciencedirect.com

ScienceDirect

ELSEVIER

Cell Type-Specific Cleavage of Nucleocapsid Protein by Effector Caspases during SARS Coronavirus Infection

Claudia Diemer, Martha Schneider, Judith Seebach, Janine Quaas, Gert Frösner, Hermann M. Schätzl* and Sabine Gilch

Institute of Virology, Technical University of Munich, Trogerstr. 30, 81675 Munich, Germany

Received 12 August 2007; received in revised form 20 November 2007; accepted 26 November 2007
Available online
4 December 2007

The epidemic outbreak of severe acute respiratory syndrome (SARS) in 2003 was caused by a novel coronavirus (CoV), designated SARS-CoV. The RNA genome of SARS-CoV is complexed by the nucleocapsid protein (N) to form a helical nucleocapsid. Besides this primary function, N seems to be involved in apoptotic scenarios. We show that upon infection of Vero E6 cells with SARS-CoV, which elicits a pronounced cytopathic effect and a high viral titer, N is cleaved by caspases. In contrast, in SARS-CoV-infected Caco-2 cells, which show a moderate cytopathic effect and a low viral titer, this processing of N was not observed. To further verify these observations, we transiently expressed N in different cell lines. Caco-2 and N2a cells served as models for persistent SARS-CoV infection, whereas Vero E6 and A549 cells did as prototype cell lines lytically infected by SARS-CoV. The experiments revealed that N induces the intrinsic apoptotic pathway, resulting in processing of N at residues 400 and 403 by caspase-6 and/or caspase-3. Of note, caspase activation is highly cell type specific in SARS-CoV-infected as well as transiently transfected cells. In Caco-2 and N2a cells, almost no N-processing was detectable. In Vero E6 and A549 cells, a high proportion of N was cleaved by caspases. Moreover, we examined the subcellular localization of SARS-CoV N in these cell lines. In transfected Vero E6 and A549 cells, SARS-CoV N was localized both in the cytoplasm and nucleus, whereas in Caco-2 and N2a cells, nearly no nuclear localization was observed. In addition, our studies indicate that the nuclear localization of N is essential for its caspase-6-mediated cleavage. These data suggest a correlation among the replication cycle of SARS-CoV, subcellular localization of N, induction of apoptosis, and the subsequent activation of caspases leading to cleavage of N.

Keywords: SARS; coronavirus; nucleocapsid protein; caspase-6; intrinsic apoptotic pathway

Edited by J. Kam

Introduction

In 2003, a novel and extremely severe respiratory disease spread worldwide from China and was denoted as severe acute respiratory syndrome (SARS). The etiologic agent associated with the clinical disease pattern was quickly identified to be a novel coronavirus (CoV) denominated SARS-CoV.[1,2] CoVs are enveloped viruses harbouring a positive-strand RNA genome.[3] Like all other CoVs, SARS-CoV encodes four structural proteins—the membrane, envelope, spike, and nucleocapsid protein (N) proteins. In addition, nine predicted unique open reading frames (ORFs) of proteins with primarily

*Corresponding author. E-mail address: schaetzl@lrz.tum.de.

Abbreviations used: SARS, severe acute respiratory syndrome; CoV, coronavirus; N, nucleocapsid protein; ORF, open reading frame; MHV, murine hepatitis virus; p.i., post-infection; NLS, nuclear localization signal; CI, caspase inhibitor; NH_4Cl, ammonium chloride; LC, lactacystin; wt, wild type; TGEV, transmissible gastroenteritis coronavirus; PBS, phosphate-buffered saline.

mostly unknown function are encoded within the 3′ end of the genome.[4,5] However, it is already known that ORF7a and ORF3a are involved in the induction of apoptosis.[6–9] ORF6 and ORF3b, as well as N, inhibit interferon-β synthesis.[10] Furthermore, ORF3a forms an ion channel, thereby enhancing virus release.[11] Before the identification of SARS-CoV, CoVs were classified into three groups (I–III). Upon phylogenetic analysis, SARS-CoV was shown to belong to the novel group IV,[4,5] with a distant relationship to group II CoVs, including members such as the human CoV OC-43 and the murine hepatitis virus (MHV).[12–14]

The RNA genome of CoVs, with about 30 kb in length, the largest known viral RNA genome, is organized by the N protein, which can dimerize via a C-terminal interaction domain.[15,16] Expression of N is essential for the packaging of viral RNA into virus-like particles,[17] and N interacts with the membrane protein in order to fix the N to the viral envelope. Besides its implication in viral assembly, SARS-CoV N appears to fulfil other important tasks in the viral life cycle and pathogenesis of SARS. In several studies, it has been shown to interfere with cellular signalling pathways.[18,19] Expression of N induces apoptosis in COS-1 cells[20,21] and leads to the activation of nuclear factor-κB in a highly cell type-dependent manner,[22] up-regulation of COX-2 activity,[23] and activation of interleukin-6 expression.[24]

One unique feature of SARS-CoV N is the presence of a lysine-rich stretch near the C-terminus of the protein, which might enable its nuclear localization.[4] Furthermore, two additional putative nuclear localization signals (NLSs) within N have been suggested, with one located at the N-terminal and the other at the middle part of the protein. Nevertheless, the localization of N within the nucleus upon transfection or infection of cells with SARS-CoV is still controversially discussed,[25–29] whereas targeting of N proteins from different CoVs to the nucleus and to nucleoli had been described.[30,31] Recently, angiotensin-converting enzyme 2 was identified as the cellular receptor for SARS-CoV.[32] Like for other human CoVs, the infection of different cell types with SARS-CoV can either be lytic or lead to viral persistence.[33–36] Specifically, the African green monkey cell line Vero E6 undergoes rapid lysis upon infection, but viral persistence can be established.[33,34] In contrast, colonic cancer cells and neuronal cells are persistently infected by SARS-CoV.[35,36]

Here we demonstrate that SARS-CoV N serves as a substrate for caspase-mediated cleavage upon viral infection or transient transfection into different cell lines, similar to the N protein of the porcine transmissible gastroenteritis CoV.[37] Interestingly, for the first time, we found in our analysis that this caspase cleavage is highly cell line dependent. Furthermore, it correlates with nuclear localization of N, shown by biochemical methods and immunocytochemistry. Altogether, our data might indicate an important possible link among nuclear localization, activation of caspases, and mechanisms for lytic *versus* persistent infection of cells with SARS-CoV.

Results

SARS-CoV N is proteolytically cleaved in a cell type-dependent manner

In order to get further insight into the cellular function of SARS-CoV N, we analysed its expression pattern in different cell lines infected with SARS-CoV or transiently transfected with N. For infection, we chose Caco-2 and Vero E6 cells and verified their susceptibility and the respective propagation of SARS-CoV on the second day post-infection (p.i.). We found that the titer of SARS-CoV propagated on Caco-2 cells was significantly lower (6.5×10^4 pfu/ml) than the titer of infected Vero E6 cells (1.8×10^6 pfu/ml). Consequently, we used Caco-2 and Vero E6 cells as a model for persistent and that for more lytic SARS-CoV infection, respectively. We inoculated both cell lines with SARS-CoV, lysed them on days 1, 2, and 3 p.i., and subjected the lysates to immunoblot analysis. Interestingly, depending on the cell line, we found only one N-specific band corresponding to the expected full-length size of 46 kDa or, in addition, a slightly faster-migrating band (indicated by an arrow in Fig. 1). In SARS-CoV-infected Vero E6 cells, we found full-length N and an additional N-specific signal at each time point of lysis (Fig. 1a). In SARS-CoV-infected Caco-2 cells, however, at any time point of lysis, only the full-length signal of N was detectable (Fig. 1b).

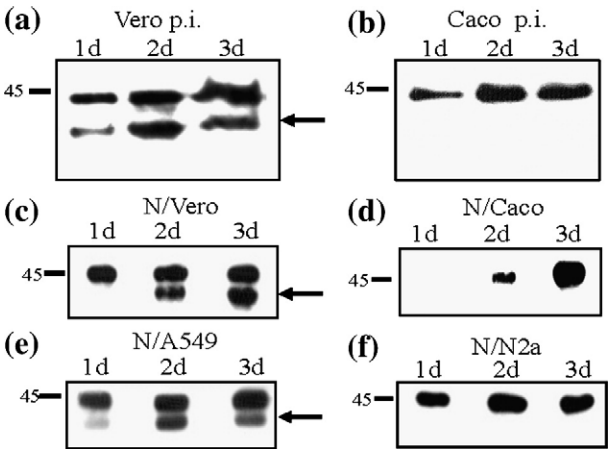

Fig. 1. SARS-CoV N processing in infected and transfected cell lines. Vero E6 (a) and Caco-2 (b) cells were infected with SARS-CoV and lysed 1, 2, or 3 days p.i. The lysates were subjected to immunoblot analysis using a polyclonal anti-N antiserum. SARS-CoV N was transiently transfected into Vero E6 (c), Caco-2 (d) A549 (e), or N2a (f) cells. Cells were lysed 1, 2, or 3 days after transfection, and lysates were analysed in immunoblot as described above. Identical results were obtained using additional polyclonal antisera (rabbit and human; data not shown). Molecular size markers are given on the left; arrows indicate the proteolytic cleavage product.

To analyse whether this expression pattern of N in different cell lines is only occurring during viral infection, we transiently expressed N in the same cell lines used for infection. Additionally, we utilized the SARS-CoV permissive human epithelial lung carcinoma cell line A549 and the murine neuronal cell line N2a to expand the models of persistent and lytic infections. Similar to Caco-2 cells, infection of neural cell lines[35] with SARS-CoV reveals low or inapparent cytopathic effects. We lysed the N-transfected cell lines on days 1, 2, and 3 after transfection and analysed the lysates in immunoblot. Interestingly, we found a cell type-specific processing of N again. In Vero E6 (Fig. 1c) and A549 (Fig. 1e) cells, both forms of N were detectable, whereas in Caco-2 (Fig. 1d) and N2a (Fig. 1f) cells, only the full-length band was observed.

In summary, we show that in SARS-CoV-infected Vero E6 cells as well as in transiently transfected A549 and Vero E6 cells, two N-specific bands were detectable, indicative for proteolytical cleavage. In contrast, in infected or transfected Caco-2 and N2a cells, only full-length N was found.

SARS-CoV N is cleaved by caspases

Depending on the cell line used, we had found an additional band to the full-length 46-kDa signal of N in infected as well as in N-transfected cell lines. In order to test whether this form was generated by proteolytical cleavage, we initially used various protease and caspase inhibitors (CIs) to decipher the responsible proteases. SARS-CoV N-transfected Vero E6 cells were mock treated or treated with ammonium chloride (NH_4Cl), lactacystin (LC), or a cell-permeable pan-CI, and lysates were analysed in immunoblot. Whereas treatment with the lysosomal inhibitor NH_4Cl and the proteasome inhibitor LC showed no effect, full-length N was detectable upon pan-CI treatment (Fig. 2a), which prevents activation of caspase-1- and caspase-3-related caspases. This indicates that the lower band is the result of caspase-mediated cleavage. Inhibition of caspase-3-related caspases prevents the activity of effector caspases-3, -6, and -7, which are the executors of apoptosis at the end of the caspase cascade. To define now which effector caspase caused the N processing, we used similar conditions as described in Fig. 2a, now using cell-permeable caspase-3- and caspase-6-specific inhibitors. As found before, mock-, NH_4Cl-, or LC-treated cells still revealed cleavage of N. However, cells treated with caspase-3 inhibitor (CI-3, Fig. 2b) or CI-6 (Fig. 2c) showed only the full-length signal of N, indicating that N processing is mediated directly by caspase-6 and caspase-3 or indirectly by activation of caspase-6 by caspase-3.

To ensure that the processing of N in virus-infected cells is also caused by caspases, we mock treated and treated SARS-CoV-infected Vero E6 cells with pan-CI (Fig. 2d) or CI-6 (Fig. 2e). Again, we found an inhibition of N processing with both inhibitors. Furthermore, we confirmed our observation that caspase-6 is cell type specifically activated

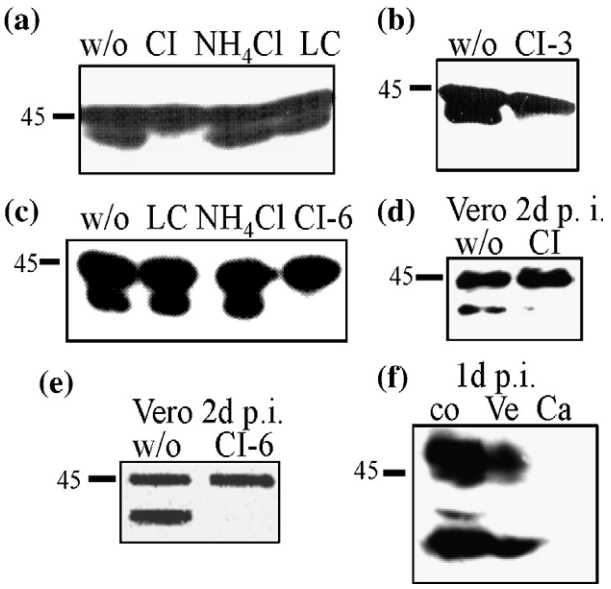

Fig. 2. Effector caspases are mediating the N cleavage. Vero E6 cells were transiently transfected with SARS-CoV N as described above. Before harvesting, cells were treated with 10 mM NH_4Cl (a and c), 2 μM LC (a and c), 100 μM z-VAD-FMK (CI) (a), 100 μM z-DEVD-FMK (CI-3) (b), or 100 μM z-VEID-FMK (CI-6) (c) or left untreated (w/o). For studies upon infection, Vero E6 cells were inoculated with SARS-CoV and treated with 100 μM z-VAD-FMK (CI) (d) or 100 μM z-VEID-FMK (CI-6) (e) or left untreated (w/o). Lysis occurred after treatment for 15 h, and lysates were analysed in immunoblot as described above. SARS-CoV-infected Vero E6 (Ve) and Caco-2 (Ca) cells or staurosporine-treated cells (co) were lysed 1 day p.i. and were subjected to immunoblot analysis using anti-cleaved lamin A antibodies (f).

during SARS-CoV infection by analysing cell lysates with a specific antibody against cleaved lamin A/C. Lamin A is the main target of caspase-6 and is cleaved by this caspase in one of the final execution steps of apoptosis.[38] Therefore, we infected Vero E6 and Caco-2 cells with SARS-CoV and lysed cells 1 day p.i. In parallel, we treated Vero E6 cells with staurosporine as a positive control (Fig. 2f). After analysis of the lysates by immunoblotting, we only found a signal for cleaved lamin A/C in staurosporine-treated and SARS-CoV-infected Vero E6 cells.

With all these data taken together, the cell type-specific cleavage of N can be prevented by both CI-6 and CI-3. Proteolysis of the caspase-6-specific substrate lamin A in infected Vero E6 but not in infected Caco-2 cells indicates activity of caspase-6 in certain infected cell lines.

Caspase-6 is activated through the intrinsic pathway and mediates C-terminal cleavage of SARS-CoV N at residues 400 and 403

Next we wanted to characterize the caspase-6 cleavage site in N and were interested in whether the caspase-6-mediated cleavage of SARS-CoV N is correlated with the subcellular localization of N. It

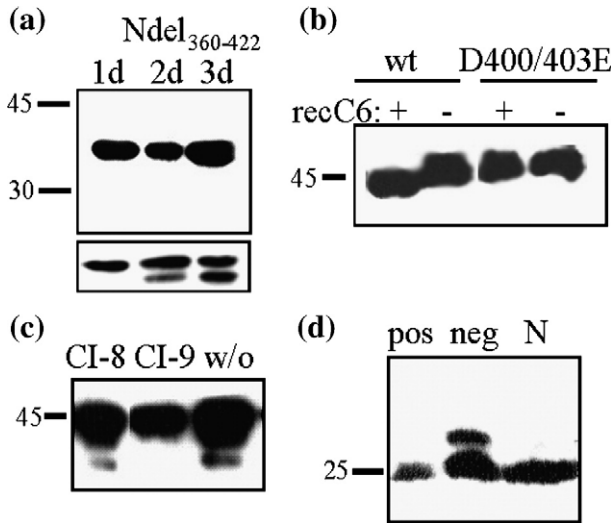

Fig. 3. Caspase-6 cleaves C-terminal residues 400 and 403 of N by activation of the intrinsic apoptotic pathway. A C-terminally truncated N mutant ($Ndel_{360–422}$) was expressed in Vero E6 cells. Cells were lysed on days 1, 2, and 3 post-transfection and analysed in immunoblot (a). The inlet picture shows the situation for cells transfected in parallel with wt N. For *in vitro* caspase-6 cleavage assay, recombinant wt N and a double-substitution mutant (D400/403E) were each incubated with recombinant caspase-6 (+) or assay buffer (−). Cleavage of protein was investigated by immunoblotting (b). N-transfected Vero E6 cells were treated with 100 μM z-LEHD-FMK (CI-9) or 100 μM z-IETD-FMK (CI-8) or left untreated. Cell lysates were analysed in immunoblot (c). COS-1 cells were transfected with N or empty vector (neg) or were treated with staurosporine (pos) and lysed 3 days after transfection. Lysates were analysed using anti-Bad antibodies in immunoblot (d).

was reported that one of the three predicted NLSs within SARS-CoV N is encoded at the C-terminal part.[25,26,39] Therefore, we generated an N mutant by deletion of C-terminal residues 360–422 (termed Ndel), which may serve as a cytosolic retention mutant and/or not be cleaved anymore. The mutant was expressed in Vero E6, and cells were each lysed 1, 2, and 3 days post-transfection. Immunoblot analysis showed a signal of the expected size of ~37 kDa. This mutant protein was found in both the cytosol and nucleus (data not shown), indicating that the deleted element was not the predominant NLS. Importantly, we could not detect an additional cleavage product at any time point (Fig. 3a), suggesting that the caspase cleavage site is likely to be embedded at the C-terminal region of N.

Caspases are aspartate-specific cysteine proteases with the cleavage occurring after aspartate residues. Since the analysis of the C-terminal deletion mutant (Fig. 3a) suggested that this region of N contains the caspase cleavage site, we examined this domain for aspartates that could constitute the putative cleavage site. Consequently, two aspartate residues were exchanged by site-directed mutagenesis to glutamates. This substitution mutant, designated D400/403E, and full-length N were expressed in *Escherichia coli* and purified. Both purified recombinant proteins were incubated in caspase activation buffer with recombinant caspase-6 (or left without caspase-6) for 3 h at 37 °C. Then, the proteins were analysed by immunoblotting. Treatment of wild-type (wt) N with caspase-6 resulted in a signal shift to a lower molecular weight compared with untreated N, indicating that recombinant caspase-6 completely processed wt N. In contrast, the substitution mutant (D400/403E) showed a signal with the same size as that for uncleaved wt N, suggesting that the caspase-6 cleavage site was in fact destroyed by the double mutation (Fig. 3b).

There are two pathways for activation of effector caspases: the extrinsic and intrinsic apoptosis pathways. In the extrinsic cascade, caspase-8 plays a crucial role; in the intrinsic pathway, caspase-9 does. To investigate which pathway is activated by N, we treated SARS-CoV N-transfected Vero E6 cells with inhibitors of these two initiator caspases or mock treated the cells for 15 h and analysed the lysates by immunoblotting (Fig. 3c). CI-9 inhibition prevented cleavage of N. In contrast, in CI-8-treated cells, cleavage of N still occurred comparable with mock-treated controls. This indicates that the intrinsic apoptotic pathway is triggered by N, resulting in activation of initiator caspase-9 and subsequent activation of effector caspases-3 and -6.

To confirm this observation, we investigated the phosphorylation state of the BH3-only protein Bad, which is activated in the intrinsic apoptotic pathway by de-phosphorylation. Therefore, we transiently transfected COS-1 cells with N or an empty vector and treated cells with staurosporine as a positive control. Three days post-transfection, we analysed the lysates by immunoblotting. We found only one signal for Bad in the positive control and in N-transfected cells, indicating complete de-phosphorylation. In the negative control (Fig. 3d), however, we detected two signals. These data show that N, as well as the commonly used apoptosis inducer staurosporine, can cause de-phosphorylation of Bad.

With all these data taken together, we show that SARS-CoV N induces the intrinsic apoptotic pathway through de-phosphorylation of Bad and activation of caspase-9, resulting in processing of N by caspases. Once caspase-6 is activated, it mediates the C-terminal cleavage of N at residues 400 and 403.

Subcellular localization of SARS-CoV N in different cell lines

Since we had found a cell type-specific processing of N by caspase-6, we asked whether there are differences in the subcellular localization of N and performed nuclear and cytosolic fractionation assays. Nuclear fractions were separated from cytosolic fractions on days 1–3 post-transfection of Vero E6, A549, Caco-2, and N2a cells and analysed in immunoblot. N is localized in both the cytoplasm and nucleus in Vero E6 (Fig. 4a, left panel) as well as A549 (Fig. 4b, left panel) cells. In Vero E6 cells,

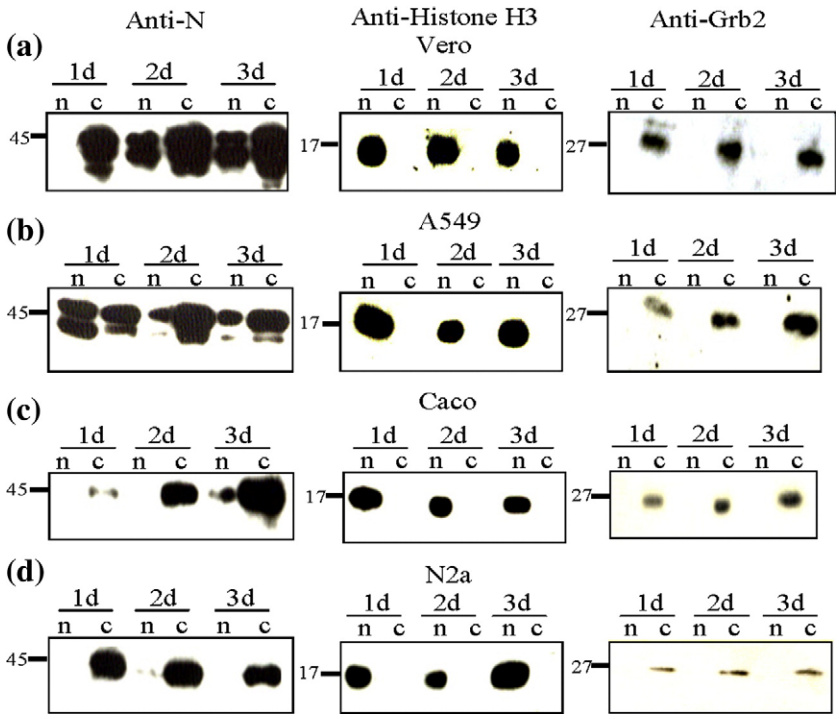

Fig. 4. Nuclear and cytosolic fractions of N-transfected cells. Nuclear and cytosolic fractions of N-transfected Vero E6 (a), A549 (b), Caco-2 (c), and N2a (d) cells were separated at different time points [1 day (1d), 2 days (2d), and 3 days (3d)] post-transfection. The fractions were analysed with the polyclonal serum against N (left panel) in immunoblot. Anti-histone H3 (middle panel) and anti-Grb2 (right panel) antibodies were used as controls for purity of the nuclear and cytosolic fractions.

nuclear localization of N was observed on the second day after transfection; in A549 cells, even on the first day after transfection. Moreover, both forms of N, full-length and cleaved N, were detected in the nucleus. In contrast, in Caco-2 cells (Fig. 4c, left panel), N is barely localized in the nucleus. A similar subcellular N localization was observed in N2a cells (Fig. 4d, left panel). Here, N was exclusively found in the cytoplasm.

To exclude contamination between nuclear and cytosolic fractions, we analysed lysates with anti-histone H3 in immunoblot. Histone H3 is known to stabilize the DNA in the nucleus and is excluded from the cytoplasm. We only detected signals in the nuclear fractions, indicating that there is no nuclear contamination of cytosolic fractions (Fig. 4a–d, middle panel). The immunoblot was re-probed with anti-Grb2 as a cytosol marker, to exclude contamination of the nuclear fraction by cytosolic proteins. As expected, we only detected signals in the cytosolic fractions (Fig. 4a–d, right panel), confirming the purity of the nuclear fractions.

In order to confirm the biochemical data, we studied the subcellular localization of N in A549, Vero E6, N2a, and Caco-2 cells by indirect immunofluorescence assay and confocal microscopy (Fig. 5). On the second (data not shown) and third days post-transfection, N was stained with anti-N polyclonal antibody, followed by cy3-labeled goat anti-rabbit antibody. For visualization of nuclei, 4′,6-diamidino-2-phenylindole staining was used. N was predominantly localized in the cytoplasm in all of the examined cell lines. However, on the second and third days post-transfection, N was found in the nucleus in ~5–10% of transfected Vero E6 and A549 cells (Fig. 5a and b). In contrast to the nuclear localization of N in A549 and Vero E6 cells, N was exclusively localized in the cytoplasm in Caco-2 and N2a cells (Fig. 5c and d).

In summary, we show by subcellular fractionation and immunofluorescence assays that N was localized in the cytoplasm of all investigated cell lines. Only in cell lines exhibiting a high cytopathic effect, which notably also show the cleavage of N, was a significant amount of both full-length and cleaved N detected in the nucleus, indicating that cleavage of N and subcellular localization are correlated.

Mutation of the NLS at residues 257–265 prevents cleavage of N

The SARS-CoV N primary sequence reveals three potential NLSs.[25] The N-terminal region of N contains a pat-7 motif (amino acids 38–44), the middle harbours pat-4 and pat-7 sequences (amino acids 257–265), and, finally, the C-terminal domain exhibits two bipartite motifs, two pat-7 motifs, and one pat-4 motif (amino acids 369–390) (Fig. 6a). To determine the main NLS of N, we first deleted the C-terminal NLS (360–422), including the five motifs. This deletion had no effect on the nuclear localization of SARS-CoV N (data not shown), however. Therefore, we investigated the NLS in the middle of N and substituted three lysines at positions 257,

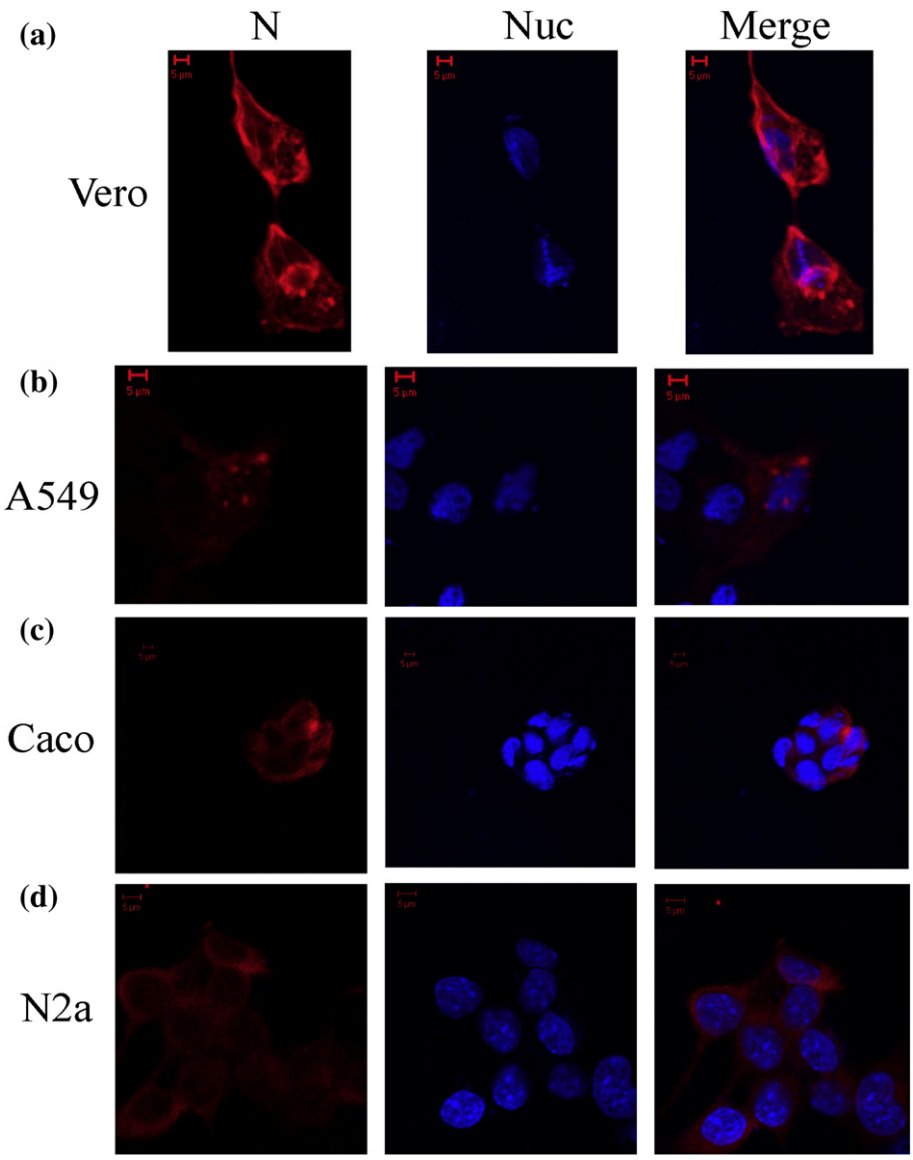

Fig. 5. Subcellular localization of SARS-CoV N. For immunofluorescence assay, Vero E6 (a), A549 (b), Caco-2 (c), and N2a (d) cells were transiently transfected with SARS-CoV N. After permeabilization, N (red) was stained with a polyclonal serum against N and with cy3-conjugated goat anti-rabbit antibody (left panel) in the different cell lines. In the middle panel, the nuclei (blue) of cells were visualized by 4′,6-diamidino-2-phenylindole staining. The merge of both stainings is shown in the right panel.

258, and 262 with glycins (NLSII; Fig. 6b). Lysines mediate the transport into the nucleus by binding to importins. To test whether this NLS is mainly responsible for the nuclear localization of N, we transiently transfected Vero E6 cells with the NLS substitution mutant (NLSII) and with wt N as a control (Fig. 6c). On days 2 and 3 post-transfection, a nuclear fractionation assay was performed. In contrast to wt N, the substitution mutant (NLSII) did not localize to the nucleus. Moreover, only the uncleaved full-length signal for NLSII was detectable, strongly indicating a correlation between nuclear localization and processing of N. Although it was already demonstrated by immunofluorescence analysis in a previous study that the NLSII sequence of SARS-CoV is a general NLS,[26] we investigated whether we can confirm this by nuclear fractionation assay. Therefore, we fused the NLSII sequence to the N-terminus of the cytosolic protein Grb2 (NLSII-Grb2) and expressed it as well as Grb2 in Vero E6 cells. Two days after transfection, we separated the nuclear and cytosolic fractions and analysed them with anti-Grb2 antibodies in immunoblot. In contrast to the nuclear fraction of Grb2, we detected a signal in the nuclear fraction of NLSII-Grb2 (Fig. 6d), indicating that NLSII is a functional NLS. To confirm the observation that the activation of apoptotic pathways correlates with nuclear localization of N, we investigated the activation of Bad under the same conditions as previously described (Fig. 3d). Therefore, we transiently transfected cells with N and NLSII. Three days post-transfection, cells were lysed and analysed with an anti-Bad antibody by immunoblotting (Fig. 6e). We

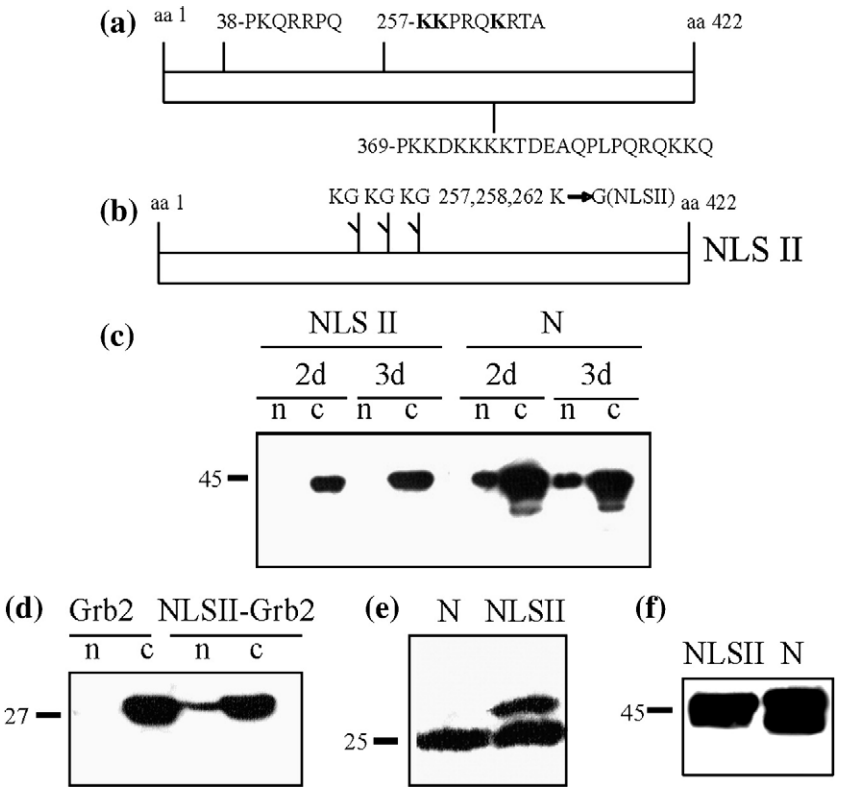

Fig. 6. Identification of the functional NLS of N. Schematic illustration of the three potential NLSs of SARS-CoV N (a) and that of the substitution mutant K257G,K258G, K262G (NLSII) of the NLS in the middle of N (b). Vero E6 cells were transiently transfected with the NLS substitution mutant (NLSII) and wt N (wt). The nuclear (*n*) and cytosolic (*c*) fractions were separated on days 2 and 3 after transfection and analysed in immunoblot (c). Vero E6 cells were transiently transfected with NLSII-Grb2 or Grb2, and nuclei (*n*) and cytosol (*c*) were fractionated on day 2 after transfection and analysed in immunoblot (d). COS-1 cells were transiently transfected with N or NLSII. After lysis, the samples were analysed with anti-Bad (e) or anti-N (f) (for loading control) antibodies by immunoblotting.

detected phosphorylated and de-phosphorylated Bad in NLSII-transfected cells, in contrast to N-transfected cells containing only the de-phosphorylated form of Bad. To exclude that this effect is due to different expression levels of N and NLSII, we subjected an aliquot of the lysates to immunoblot analysis using anti-N antisera. This immunoblot analysis revealed that the expression of N and that of NLSII were nearly the same (Fig. 6f).

With all these data taken together, we could identify the predominant NLS of SARS-CoV N at residues 257–265. In addition, the experiments clearly reveal that the nuclear localization of SARS-CoV N is essential for triggering the intrinsic apoptotic pathway and for subsequent N cleavage.

Discussion

Until the outbreak of SARS, caused by SARS-CoV, two human CoVs leading to mild respiratory diseases were already known, 229E and OC-43. Since the high mortality rate upon SARS-CoV infection is striking, it is of great importance to understand viral factors or virus–host interactions that are responsible for the aggressive course of SARS. Since N accomplishes other functions besides complexing the viral genomic RNA, it might be a possible candidate in such scenarios.

Cell type differences determine pro-apoptotic potential of N

Our study on the processing of SARS-CoV N in transiently transfected and SARS-CoV-infected cells revealed that N is cleaved by caspase-6 and potentially by caspase-3. Since caspase-3 is the activator of caspase-6, inhibition of N-cleavage by CI-3 might be due to a blocked downstream activation of caspase-6. In addition, we demonstrated that the caspase-6 cleavage site is located at residues 400 and 403 of N. The N protein of transmissible gastroenteritis coronavirus (TGEV) is also cleaved by caspases during viral infection, pointing to a common feature and an important function of this processing.[37] Caspase-6 is an effector caspase that is, once activated by initiator and effector caspases, mediating the morphological changes characteristic for apoptotic cell death.[40,41] Its transactivation is regulated by p53, and induction of caspase-6 expression induces apoptotic signals that activate caspase-6.[42] Previous reports already suggested that N is a pro-apoptotic protein.[20,24,43] Accordingly, we show that N triggers the intrinsic apoptotic pathway by activation of the initiator caspase-9 as well as de-phosphorylation of pro-apoptotic Bad.

Interestingly, our examination of different SARS-CoV-infected or N-transfected cell lines demonstrated that caspase-6-mediated cleavage of N depends on the used cell line and obviously correlates with the replication cycle of SARS-CoV. N processing is only observed in cells known to be lytically infected by SARS-CoV, such as Vero E6 and A549 cells, but not in Caco-2 and N2a cells, which we used as models for persistently infected cells.[35,36] Of note, characterization of SARS-CoV pathogenesis by autopsied tissues from SARS patients revealed viral signals in the lung with severe harm, whereas in the intestine and brain, no apparent damage was

observed despite detectable amounts of SARS-CoV.[44–46] First, these give evidence that intestine and neural tissues might be persistently infected by SARS-CoV. Second, these raise the question of whether N is involved in the establishment of lytic or persistent infection. In infected Vero E6 cells, the transcription factor STAT3 is de-phosphorylated and disappears from the nucleus,[47] resulting in decreased cell viability. In N-transfected COS-1 cells, p38 MAPK and JNK as well as caspase-3 and caspase-7 are up-regulated.[20] In contrast, in persistently infected Vero E6 subclones, the anti-apoptotic proteins Bcl-2 and Bcl-XL are up-regulated. Here, transient expression of N induced phosphorylation of Akt and JNK, possibly leading to the establishment of persistence.[33] In human intestinal epithelial cells and in neurons, the PI3/Akt pathway can be involved in cell survival.[48–50] Therefore, the different regulation of survival pathways in various cell lines could account for the distinctions exhibited by N regarding activation of apoptotic pathways.

N as inducer and substrate of apoptotic execution

Many viruses evoke apoptosis in infected cells. This is also the case in SARS-CoV-infected Vero E6 cells,[18] raising the common question of whether here induction of apoptosis is host defence or is even favourable for the viral life cycle. In the case of host defence, the infected cell initiates apoptosis to inhibit spread of progeny virus or to eliminate viral proteins at the end of the apoptotic cascade. However, a growing number of viruses were shown to adapt to the host cell death machinery in order to promote spread of progeny or to utilize caspases to cleave their own proteins for benefiting viral replication or persistence.[51] CoV-induced apoptosis occurs upon infection of cells with TGEV, and here the N protein serves as substrate for caspase-6 and caspase-7.[37] In defined SARS-CoV-infected cell lines, N is also cleaved by caspases. Moreover, we show here that upon transient expression, N itself is an inducer and subsequently a substrate of caspase-6 in Vero E6 and A549 cells. This is in contrast to many other viral proteins, which either provoke or are the target of apoptosis, and suggests that caspase-6 activity and subsequent processing of N have roles during viral maturation other than simply the induction of apoptosis to fend the virus. In general, the N protein would be an appropriate target for fending of viral invasion, since this protein is necessary for viral assembly. Moreover, in the case of TGEV, only full-length N is packaged in the virion,[37] indicating that caspase-6 processing might inhibit viral assembly. On the other hand, in Vero E6 cells, high viral titers are achieved despite N cleavage. Furthermore, a caspase cleavage site occurs also in TGEV N and has not been eliminated by mutations more beneficial for the virus, suggesting an important role for the viral life cycle.

Nuclear localization of N is necessary for induction of intrinsic apoptotic pathway and N processing

We found that in lytically infected Vero E6 and A549 cells, but not in cell models for persistent infection, N was located in the nucleus. This means that only in cells exhibiting nuclear localization of N was the protein processed by caspase-6. This raises two possibilities: either N is translocated to the nucleus, leading to the induction of caspase-6 activity, or N can only be imported into the nucleus if caspase-6 is active during apoptotic processes. An example for such a mechanism is provided by the NS1 protein of Aleutian mink disease parvovirus.[52] When we analysed a mutant of N containing substitutions within the predicted NLS between residue 257 and residue 265, it was not imported into the nucleus. This demonstrates that this stretch contains a functional NLS, supported by the partial redistribution to the nucleus of transiently expressed cytosolic Grb2 fused to this NLS. Even more interesting are that the mutant was not cleaved in Vero E6 cells and Bad was not de-phosphorylated, indicating that apoptosis and, subsequently, caspase-6 were not activated. Furthermore, treatment of N-transfected Vero E6 cells with CIs did not prevent nuclear localization of N (data not shown), indicating that caspase cleavage is not necessary for nuclear import of N. This leads to the conclusion that nuclear localization of N is a prerequisite for the induction of caspase-6 activity. Of note, we found both processed and full-length N within the nucleus. This is reasonable, as the processed form of N still contains the NLS. Since caspase-6 cleaves lamin A during apoptosis, leading to an increased permeability of the nuclear pores,[51] N might also enter the nuclei of apoptotic cells non-specifically by passive diffusion. This was basically excluded by us because the cytosolic marker protein Grb2 was detectable exclusively within cytoplasmic fractions.

Nuclear import via NLS has been observed for N proteins of several other CoVs (e.g., infectious bronchitis virus, MHV,[30] and the related porcine reproductive and respiratory syndrome virus[53]). For the latter virus, deletion of the NLS of N led to a shorter viremia. Persistence of these NLS-null mutants was observed, but detailed analysis revealed that nuclear localization of N protein of these viruses was restored by point mutations within the NLS, resulting in a functional NLS.[54] In addition, some MHV strains cause fulminant hepatitis in mice, dependent on N and the infected cell type. Here, N acts as a transcription factor—not directly but in connection with a host factor.[55] These data indicate that indeed the nuclear localization of N can modulate pathogenicity of viruses.

With all these data taken together, the induction of apoptosis, leading to caspase-6-dependent processing of N, is cell type specific and might be explained by activation of survival pathways in persistently infected cells. In the case N is imported into the nucleus, apoptosis is induced via the intrinsic path-

way and, thereby, caspase-6 activation leads to the processing of N (schematically depicted in Fig. 7). Within the nucleus, N could in addition act as a transcription factor, either directly[23] or dependent on host factors. This model underlines the possibility that the nuclear localization of N might be involved in the pathogenicity of SARS-CoV.

Materials and Methods

Reagents

Antiserum against N was generated by immunization of rabbits with purified recombinant N expressed in *E. coli*. This antiserum recognizes SARS-CoV N protein specifically and was used for immunoblot and immunofluorescence analyses. Specificity of this antiserum was validated by employing another rabbit polyclonal serum generated similarly, by using two commercially available peptide-induced polyclonal antisera (Imgenex, San Diego, CA) and with a pool of human antisera obtained from SARS-infected patients (kindly provided by Dr. Peiris, Hong Kong). As secondary antibodies, horseradish peroxidase-conjugated anti-rabbit immunoglobulin G (GE Healthcare, München, Germany) in immunoblot analysis and cy3-conjugated donkey anti-rabbit immunoglobulin G (Dianova, Hamburg, Germany) in immunofluorescence assay were used. The purity of the nuclear fractions was tested by anti-histone H3 (Calbiochem, Nottingham, UK), whereas that of the cytosolic fractions was tested by anti-Grb2 (Santa Cruz, Heidelberg, Germany) after stripping with ReBlot Plus Strong Solution (Chemicon International, Hampshire, UK). Cleaved lamin A/C antibody (Cell Signaling Technology, Danvers, MA) recognizes the cleaved large fragment of lamin A/C. The anti-Bad antibody (Santa Cruz) detects the phosphorylated and de-phosphorylated forms of the BH3-only protein Bad.

Immunoblotting was done using the enhanced chemiluminescence technique (ECL Plus) and PVDF (polyvinylidene fluoride) Transfer Membrane (Hybond-P) from GE Healthcare. Pefabloc protease inhibitor was obtained from Roche (Mannheim, Germany). Cell culture media and solutions were purchased from Invitrogen (Karlsruhe, Germany). z-IETD-FMK (CI-8), z-LEHD-FMK (CI-9), and z-DEVD-FMK (CI-3) were obtained from Calbiochem; z-VAD-FMK, z-VEID-FMK, LC, staurosporine, and NH_4Cl, from Sigma-Aldrich (Munich, Germany).

Plasmid construction

The N gene was derived from SARS-CoV isolate Frankfurt-1 (kindly provided by Dr. B. Schweiger, RKI Berlin, Berlin, Germany). It was amplified by reverse transcriptase PCR and transferred by recombination into the plasmid pDest (gateway system, Invitrogen) downstream of the T7 promoter and the polyhistidine tag. The C-terminal double-substitution mutant D400/403E and the NLS K257G,K258G,K262G (NLSII) substitution mutant were generated by site-directed mutagenesis using *Pfu* DNA polymerase (Stratagene, La Jolla, CA). The NLSII sequence (amino acids 257–262) of N was engineered N-terminally to Grb2 (NLSII-Grb2) by PCR mutagenesis. Sequence analysis was always carried out to confirm the amino acid substitutions. For expression in eukaryotic cells, the full-length and all mutants were cloned into pcDNA3.1/Zeo (+) (Invitrogen).

Protein expression in *E. coli* and purification

His-tagged SARS-CoV N protein and the double-substitution mutant (D400/403E) were expressed in *E. coli* BL21 (Invitrogen) after induction with 0.02% L-arabinose. Bacterial cells were lysed (6 M GdnHCl, 20 mM Na_3PO_4, and 500 mM NaCl, pH 7.8), and lysates were loaded on a Ni–nitrilotriacetic acid affinity column (Invitrogen). After several washing steps, His-tagged proteins were recovered with elution buffer containing 8 M urea, 20 mM Na_3PO_4, and 500 mM imidazole, pH 6.3. The eluate was refolded by dialysis against sodium acetate,

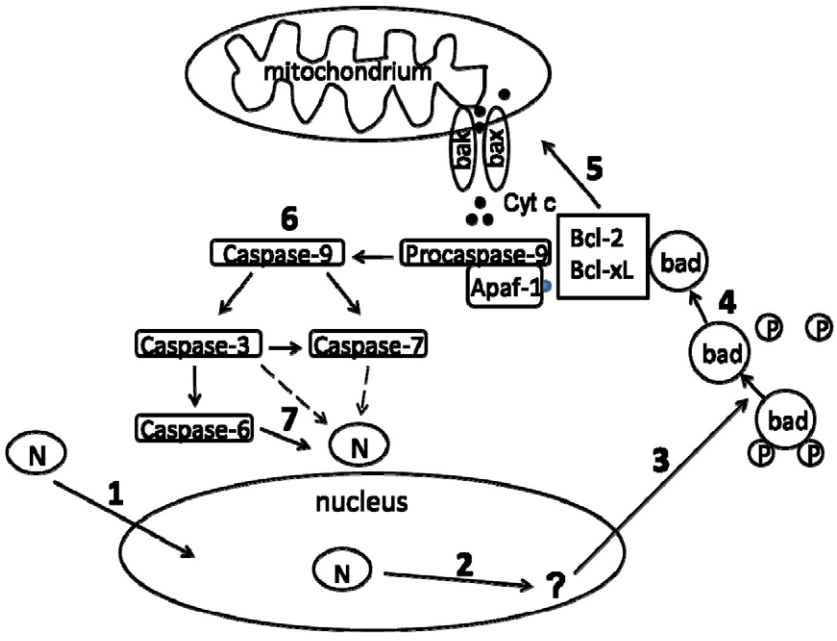

Fig. 7. Hypothetical model for correlation of nuclear localization and caspase-mediated cleavage of N in lytic SARS-CoV infection. N translocates into the nucleus (1) and may activate gene expression or interact with nuclear components there (2), resulting in the de-phosphorylation of Bad (3). In this form, Bad is enabled to interact with Bcl-2 and Bcl-XL (4). This interaction releases Bax and Bak from pro-survival Bcl-2 proteins, enabling insertion of Bax and Bak in the mitochondrial membrane. The resulting membrane permeabilization facilitates cytochrome *c* efflux (5), which provokes the activation of pro-caspase-9 by formation of apoptosome. Once caspase-9 is activated, the caspase cascade occurs and effector caspases (i.e., caspase-3, caspase-6, and caspase-7) are activated (6). Finally, N is cleaved by caspase-6 (7), but cleavage of N may additionally be caused by caspase-3 or caspase-7.

pH 5.2, and quantified by Bradford assay (Coomassie protein assay reagent, Pierce, Bonn, Germany). The purified proteins were used for immunization of rabbits and for the *in vitro* caspase-6 cleavage assay.

In vitro caspase-6 cleavage assay

Purified N or D400/403E mutant protein (125 ng) was incubated either without or with 100 ng/ml of active recombinant human caspase-6 (Mch2, BD Pharmigen, Heidelberg, Germany) in a final volume of 20 μl of caspase assay buffer [20 mM Pipes, 100 mM NaCl, 10 mM DTT, 1 mM ethylenediaminetetraacetic acid (EDTA), 0.1% (w/v) 3-[(3-cholamidopropyl)dimethylammonio]propanesulfonic acid, and 10% sucrose, pH 7.2] for 3 h at 37 °C. The reaction was terminated by the addition of gel loading buffer, and cleavage of the protein was analysed by immunoblotting.

Virus and cell culture

Vero E6 and Caco-2 cells were grown in cell culture flasks until they reached 80% confluence. The growth medium [Dulbecco's modified Eagle's medium (DMEM), 10% fetal calf serum, 100 U of penicillin, and 100 μg of streptomycin per milliliter] was removed, and the cells were inoculated with SARS-CoV (Frankfurt-1 strain) in 2 ml of infection medium (DMEM without fetal calf serum, 100 U of penicillin, and 100 μg of streptomycin per milliliter). After 1 h at 37 °C, 2 ml of growth medium was added. One, 2, and 3 days p.i., Vero E6 and Caco-2 cells were lysed, the virus supernatants of these cells were harvested, and cell debris was removed by centrifugation (700*g* for 10 min at 4 °C). For caspase inhibition, SARS-CoV-infected Vero E6 cells were treated with 100 μM z-VAD-FMK or 100 μM z-VEID-FMK 1 day p.i. and were lysed after 24 h of treatment. Virus stocks were stored at −80 °C and thawed immediately before their use for titration.

Plaque assay

Vero E6 cells were infected with dilutions of viral supernatants that were harvested from Caco-2 and Vero E6 cells on the second day p.i. After 1 h, the cells were overlaid with growth medium containing 1% methylcellulose. Forty-eight hours p.i., the overlay was removed and the cells were fixed in 4% formalin for 1 h. For cell staining, 2% crystal violet in 3.6% formaldehyde and 20% ethanol was used.

Cell culture and DNA transfection

A549 (ATCC-CCL-185), Vero E6 (ATCC-CRL-1586), and COS-1 (ATCC-CRL-1650) cell lines were maintained in DMEM, N2a cells (ATCC-CCL-131) in Optimem, and Caco-2 cells (ATCC-HTB-37) in Earle's MEM at 37 °C with 5% CO_2. The media were supplemented with 10% fetal bovine serum, 100 U of penicillin, and 100 μg of streptomycin per milliliter. A549 cells were transfected with Lipofectamine 2000 (Invitrogen), whereas N2a, COS-1 Vero E6, and Caco-2 cells were transfected with FuGENE 6 (Roche) with the pcDNA3.1 N, pcDNA3.1 NLSII, pcDNA3.1 Ndel, pcDNA3.1 Grb2, pcDNA3.1 NLSII-Grb2, or pcDNA3.1 constructs according to the manufacturer's protocol.

The inhibitors z-IETD-FMK (CI-8; 100 μM), z-LEHD-FMK (CI-9; 100 μM), z-VAD-FMK (pan-CI; 100 μM), z-VEID-FMK (CI-6; 100 μM), z-DEVD-FMK (CI-3; 100 μM), staurosporine (2.5 μM), LC (2 μM), and NH_4Cl (10 mM) were added to the cell culture medium for 15 h each before harvesting.

Nuclear extraction and cell lysis

To fractionate nuclei, we washed cells two times with phosphate-buffered saline (PBS) and incubated them in lysis buffer (40 mM Tris–HCl, pH 7.4, 150 mM NaCl, 1 mM EDTA, 0.3% Nonidet P-40, and 1 mM DTT) for 10 min on ice.[52] The nuclei were pelleted by centrifugation at 800*g* for 10 min and washed once with PBS. The supernatant containing the cytosolic fraction was precipitated with methanol. The protein amount in the nuclear fraction was quantified by Bradford assay (Pierce). For cell lysis, cells were washed with PBS and incubated in lysis buffer (10 mM Tris, pH 7.5, 100 mM NaCl, 10 mM EDTA, 0.5% Triton X-100, and 0.5% Na–desoxycholate) for 10 min. The lysates were cleared by centrifugation for 1 min at 14.000 rpm, and supernatants were precipitated with methanol. After centrifugation for 30 min at 3.500 rpm, the pellets were re-suspended in TNE buffer (50 mM Tris–HCl, pH 7.5, 150 mM NaCl, and 5 mM EDTA). Total cell lysates as well as nuclear and cytosolic fractions were analysed by 12.5% SDS-PAGE as described previously.[56]

Immunofluorescence and confocal laser-scanning microscopy

Cells were grown on glass cover slips (Marienfeld, Bad Mergentheim, Germany). On the third day post-transfection, cells were fixed with 3% paraformaldehyde in PBS for 30 min at room temperature. After sequential treatment with NH_4Cl (50 mM in 20 mM glycine), Triton X-100 (0.3% in PBS), and gelatine (0.2% in PBS) for 10 min each at room temperature, anti-N antibody (1:100 in PBS) was added and incubated for 30 min at room temperature. After an additional incubation for 30 min at room temperature with cy3-conjugated secondary antibody (Dianova, Hamburg, Germany) (1:400 in PBS), the slides were incubated with 4′,6-diamidino-2-phenylindole (Roche Applied Science, Mannheim, Germany) for 10 min. Following staining, the slides were mounted in anti-fading solution (Permafluor, Beckman Coulter, Krefeld, Germany) and stored at +4 °C. Confocal laser scanning microscopy was done using a Zeiss LSM 510 confocal system (Carl Zeiss, Jena, Göttingen, Germany).

Acknowledgements

We thank Prof. C. Drosten (Bernhard-Nocht Institute Hamburg, now Institute of Virology of the University of Bonn) for providing infectious SARS-CoV, his colleague Dr. S. Pfefferle for giving auxiliary advice on basic SARS-CoV propagation and titration, and Dr. B. Schweiger (RKI Berlin) for providing nucleic acid of SARS-CoV isolate Frankfurt-1 for initial cloning studies.

References

1. Drosten, C., Gunther, S., Preiser, W., van der, W. S., Brodt, H. R., Becker, S. *et al.* (2003). Identification of a novel coronavirus in patients with severe acute respiratory syndrome. *N. Engl. J. Med.* **348**, 1967–1976.
2. Ksiazek, T. G., Erdman, D., Goldsmith, C. S., Zaki, S. R., Peret, T., Emery, S. *et al.* (2003). A novel coronavirus associated with severe acute respiratory syndrome. *N. Engl. J. Med.* **348**, 1953–1966.
3. Ziebuhr, J. (2004). Molecular biology of severe acute respiratory syndrome coronavirus. *Curr. Opin. Microbiol.* **7**, 412–419.
4. Marra, M. A., Jones, S. J., Astell, C. R., Holt, R. A., Brooks-Wilson, A., Butterfield, Y. S. *et al.* (2003). The genome sequence of the SARS-associated coronavirus. *Science*, **300**, 1399–1404.
5. Rota, P. A., Oberste, M. S., Monroe, S. S., Nix, W. A., Campagnoli, R., Icenogle, J. P. *et al.* (2003). Characterization of a novel coronavirus associated with severe acute respiratory syndrome. *Science*, **300**, 1394–1399.
6. Law, P. T., Wong, C. H., Au, T. C., Chuck, C. P., Kong, S. K., Chan, P. K. *et al.* (2005). The 3a protein of severe acute respiratory syndrome-associated coronavirus induces apoptosis in Vero E6 cells. *J. Gen. Virol.* **86**, 1921–1930.
7. Tan, Y. J., Fielding, B. C., Goh, P. Y., Shen, S., Tan, T. H., Lim, S. G. & Hong, W. (2004). Overexpression of 7a, a protein specifically encoded by the severe acute respiratory syndrome coronavirus, induces apoptosis via a caspase-dependent pathway. *J. Virol.* **78**, 14043–14047.
8. Tan, Y. X., Tan, T. H., Lee, M. J., Tham, P. Y., Gunalan, V., Druce, J. *et al.* (2007). Induction of apoptosis by the severe acute respiratory syndrome coronavirus 7a protein is dependent on its interaction with the Bcl-XL protein. *J. Virol.* **81**, 6346–6355.
9. Kopecky-Bromberg, S. A., Martinez-Sobrido, L. & Palese, P. (2006). 7a protein of severe acute respiratory syndrome coronavirus inhibits cellular protein synthesis and activates p38 mitogen-activated protein kinase. *J. Virol.* **80**, 785–793.
10. Kopecky-Bromberg, S. A., Martinez-Sobrido, L., Frieman, M., Baric, R. A. & Palese, P. (2007). Severe acute respiratory syndrome coronavirus open reading frame (ORF) 3b, ORF 6, and nucleocapsid proteins function as interferon antagonists. *J. Virol.* **81**, 548–557.
11. Lu, W., Zheng, B. J., Xu, K., Schwarz, W., Du, L., Wong, C. K. *et al.* (2006). Severe acute respiratory syndrome-associated coronavirus 3a protein forms an ion channel and modulates virus release. *Proc. Natl Acad. Sci. USA*, **103**, 12540–12545.
12. Snijder, E. J., Bredenbeek, P. J., Dobbe, J. C., Thiel, V., Ziebuhr, J., Poon, L. L. *et al.* (2003). Unique and conserved features of genome and proteome of SARS-coronavirus, an early split-off from the coronavirus group 2 lineage. *J. Mol. Biol.* **331**, 991–1004.
13. Kim, O. J., Lee, D. H. & Lee, C. H. (2006). Close relationship between SARS-coronavirus and group 2 coronavirus. *J. Microbiol.* **44**, 83–91.
14. Eickmann, M., Becker, S., Klenk, H. D., Doerr, H. W., Stadler, K., Censini, S. *et al.* (2003). Phylogeny of the SARS coronavirus. *Science*, **302**, 1504–1505.
15. Surjit, M., Liu, B., Kumar, P., Chow, V. T. & Lal, S. K. (2004). The nucleocapsid protein of the SARS coronavirus is capable of self-association through a C-terminal 209 amino acid interaction domain. *Biochem. Biophys. Res. Commun.* **317**, 1030–1036.
16. Yu, I. M., Oldham, M. L., Zhang, J. & Chen, J. (2006). Crystal structure of the severe acute respiratory syndrome (SARS) coronavirus nucleocapsid protein dimerization domain reveals evolutionary linkage between *Corona-* and *Arteriviridae*. *J. Biol. Chem.* **281**, 17134–17139.
17. Hsieh, P. K., Chang, S. C., Huang, C. C., Lee, T. T., Hsiao, C. W., Kou, Y. H. *et al.* (2005). Assembly of severe acute respiratory syndrome coronavirus RNA packaging signal into virus-like particles is nucleocapsid dependent. *J. Virol.* **79**, 13848–13855.
18. Mizutani, T., Fukushi, S., Saijo, M., Kurane, I. & Morikawa, S. (2004). Phosphorylation of p38 MAPK and its downstream targets in SARS coronavirus-infected cells. *Biochem. Biophys. Res. Commun.* **319**, 1228–1234.
19. He, R., Leeson, A., Andonov, A., Li, Y., Bastien, N., Cao, J. *et al.* (2003). Activation of AP-1 signal transduction pathway by SARS coronavirus nucleocapsid protein. *Biochem. Biophys. Res. Commun.* **311**, 870–876.
20. Surjit, M., Liu, B., Jameel, S., Chow, V. T. & Lal, S. K. (2004). The SARS coronavirus nucleocapsid protein induces actin reorganization and apoptosis in COS-1 cells in the absence of growth factors. *Biochem. J.* **383**, 13–18.
21. Zhang, L., Wei, L., Jiang, D., Wang, J., Cong, X. & Fei, R. (2007). SARS-CoV nucleocapsid protein induced apoptosis of COS-1 mediated by the mitochondrial pathway. *Artif. Cells, Blood Substitutes, Immobilization Biotechnol.* **35**, 237–253.
22. Liao, Q. J., Ye, L. B., Timani, K. A., Zeng, Y. C., She, Y. L., Ye, L. & Wu, Z. H. (2005). Activation of NF-kappaB by the full-length nucleocapsid protein of the SARS coronavirus. *Acta Biochim. Biophys. Sin.* **37**, 607–612.
23. Yan, X., Hao, Q., Mu, Y., Timani, K. A., Ye, L., Zhu, Y. & Wu, J. (2006). Nucleocapsid protein of SARS-CoV activates the expression of cyclooxygenase-2 by binding directly to regulatory elements for nuclear factor-kappa B and CCAAT/enhancer binding protein. *Int. J. Biochem. Cell Biol.* **38**, 1417–1428.
24. Zhang, X., Wu, K., Wang, D., Yue, X., Song, D., Zhu, Y. & Wu, J. (2007). Nucleocapsid protein of SARS-CoV activates interleukin-6 expression through cellular transcription factor NF-kappaB. *Virology*, **365**, 324–335.
25. Rowland, R. R., Chauhan, V., Fang, Y., Pekosz, A., Kerrigan, M. & Burton, M. D. (2005). Intracellular localization of the severe acute respiratory syndrome coronavirus nucleocapsid protein: absence of nucleolar accumulation during infection and after expression as a recombinant protein in Vero cells. *J. Virol.* **79**, 11507–11512.
26. You, J., Dove, B. K., Enjuanes, L., Dediego, M. L., Alvarez, E., Howell, G. *et al.* (2005). Subcellular localization of the severe acute respiratory syndrome coronavirus nucleocapsid protein. *J. Gen. Virol.* **86**, 3303–3310.
27. Timani, K. A., Liao, Q., Ye, L., Zeng, Y., Liu, J., Zheng, Y. *et al.* (2005). Nuclear/nucleolar localization properties of C-terminal nucleocapsid protein of SARS coronavirus. *Virus Res.* **114**, 23–34.
28. Surjit, M., Kumar, R., Mishra, R. N., Reddy, M. K., Chow, V. T. & Lal, S. K. (2005). The severe acute respiratory syndrome coronavirus nucleocapsid protein is phosphorylated and localizes in the cytoplasm by 14-3-3-mediated translocation. *J. Virol.* **79**, 11476–11486.
29. You, J. H., Reed, M. L. & Hiscox, J. A. (2007). Trafficking motifs in the SARS-coronavirus nucleo-

capsid protein. *Biochem. Biophys. Res. Commun.* **358**, 1015–1020.
30. Wurm, T., Chen, H., Hodgson, T., Britton, P., Brooks, G. & Hiscox, J. A. (2001). Localization to the nucleolus is a common feature of coronavirus nucleoproteins, and the protein may disrupt host cell division. *J. Virol.* **75**, 9345–9356.
31. Hiscox, J. A., Wurm, T., Wilson, L., Britton, P., Cavanagh, D. & Brooks, G. (2001). The coronavirus infectious bronchitis virus nucleoprotein localizes to the nucleolus. *J. Virol.* **75**, 506–512.
32. Li, W., Moore, M. J., Vasilieva, N., Sui, J., Wong, S. K., Berne, M. A. *et al.* (2003). Angiotensin-converting enzyme 2 is a functional receptor for the SARS coronavirus. *Nature*, **426**, 450–454.
33. Mizutani, T., Fukushi, S., Ishii, K., Sasaki, Y., Kenri, T., Saijo, M. *et al.* (2006). Mechanisms of establishment of persistent SARS-CoV-infected cells. *Biochem. Biophys. Res. Commun.* **347**, 261–265.
34. Yamate, M., Yamashita, M., Goto, T., Tsuji, S., Li, Y. G., Warachit, J. *et al.* (2005). Establishment of Vero E6 cell clones persistently infected with severe acute respiratory syndrome coronavirus. *Microbes Infect.* **7**, 1530–1540.
35. Yamashita, M., Yamate, M., Li, G. M. & Ikuta, K. (2005). Susceptibility of human and rat neural cell lines to infection by SARS-coronavirus. *Biochem. Biophys. Res. Commun.* **334**, 79–85.
36. Chan, P. K., To, K. F., Lo, A. W., Cheung, J. L., Chu, I., Au, F. W. *et al.* (2004). Persistent infection of SARS coronavirus in colonic cells *in vitro*. *J. Med. Virol.* **74**, 1–7.
37. Eleouet, J. F., Slee, E. A., Saurini, F., Castagne, N., Poncet, D., Garrido, C. *et al.* (2000). The viral nucleocapsid protein of transmissible gastroenteritis coronavirus (TGEV) is cleaved by caspase-6 and -7 during TGEV-induced apoptosis. *J. Virol.* **74**, 3975–3983.
38. Ruchaud, S., Korfali, N., Villa, P., Kottke, T. J., Dingwall, C., Kaufmann, S. H. & Earnshaw, W. C. (2002). Caspase-6 gene disruption reveals a requirement for lamin A cleavage in apoptotic chromatin condensation. *EMBO J.* **21**, 1967–1977.
39. Li, F. Q., Xiao, H., Tam, J. P. & Liu, D. X. (2005). Sumoylation of the nucleocapsid protein of severe acute respiratory syndrome coronavirus. *FEBS Lett.* **579**, 2387–2396.
40. Stennicke, H. R. & Salvesen, G. S. (1998). Properties of the caspases. *Biochim. Biophys. Acta*, **1387**, 17–31.
41. Bratton, S. B., MacFarlane, M., Cain, K. & Cohen, G. M. (2000). Protein complexes activate distinct caspase cascades in death receptor and stress-induced apoptosis. *Exp. Cell Res.* **256**, 27–33.
42. MacLachlan, T. K. & El Deiry, W. S. (2002). Apoptotic threshold is lowered by p53 transactivation of caspase-6. *Proc. Natl Acad. Sci. USA*, **99**, 9492–9497.
43. Zhao, G., Shi, S. Q., Yang, Y. & Peng, J. P. (2006). M and N proteins of SARS coronavirus induce apoptosis in HPF cells. *Cell Biol. Toxicol.* **22**, 313–322.
44. Ding, Y., He, L., Zhang, Q., Huang, Z., Che, X., Hou, J. *et al.* (2004). Organ distribution of severe acute respiratory syndrome (SARS) associated coronavirus (SARS-CoV) in SARS patients: implications for pathogenesis and virus transmission pathways. *J. Pathol.* **203**, 622–630.
45. To, K. F., Tong, J. H., Chan, P. K., Au, F. W., Chim, S. S., Chan, K. C. *et al.* (2004). Tissue and cellular tropism of the coronavirus associated with severe acute respiratory syndrome: an *in-situ* hybridization study of fatal cases. *J. Pathol.* **202**, 157–163.
46. To, K. F. & Lo, A. W. (2004). Exploring the pathogenesis of severe acute respiratory syndrome (SARS): the tissue distribution of the coronavirus (SARS-CoV) and its putative receptor, angiotensin-converting enzyme 2 (ACE2). *J. Pathol.* **203**, 740–743.
47. Mizutani, T., Fukushi, S., Murakami, M., Hirano, T., Saijo, M., Kurane, I. & Morikawa, S. (2004). Tyrosine dephosphorylation of STAT3 in SARS coronavirus-infected Vero E6 cells. *FEBS Lett.* **577**, 187–192.
48. Gauthier, R., Harnois, C., Drolet, J. F., Reed, J. C., Vezina, A. & Vachon, P. H. (2001). Human intestinal epithelial cell survival: differentiation state-specific control mechanisms. *Am. J. Physiol.: Cell Physiol.* **280**, C1540–C1554.
49. Franke, T. F., Kaplan, D. R. & Cantley, L. C. (1997). PI3K: downstream AKTion blocks apoptosis. *Cell*, **88**, 435–437.
50. Vemuri, G. S. & McMorris, F. A. (1996). Oligodendrocytes and their precursors require phosphatidylinositol 3-kinase signaling for survival. *Development*, **122**, 2529–2537.
51. Best, S. M. & Bloom, M. E. (2004). Caspase activation during virus infection: more than just the kiss of death? *Virology*, **320**, 191–194.
52. Best, S. M., Shelton, J. F., Pompey, J. M., Wolfinbarger, J. B. & Bloom, M. E. (2003). Caspase cleavage of the nonstructural protein NS1 mediates replication of Aleutian mink disease parvovirus. *J. Virol.* **77**, 5305–5312.
53. Rowland, R. R., Kervin, R., Kuckleburg, C., Sperlich, A. & Benfield, D. A. (1999). The localization of porcine reproductive and respiratory syndrome virus nucleocapsid protein to the nucleolus of infected cells and identification of a potential nucleolar localization signal sequence. *Virus Res.* **64**, 1–12.
54. Lee, C., Hodgins, D., Calvert, J. G., Welch, S. K., Jolie, R. & Yoo, D. (2006). Mutations within the nuclear localization signal of the porcine reproductive and respiratory syndrome virus nucleocapsid protein attenuate virus replication. *Virology*, **346**, 238–250.
55. Ning, Q., Lakatoo, S., Liu, M., Yang, W., Wang, Z., Phillips, M. J. & Levy, G. A. (2003). Induction of prothrombinase *fgl2* by the nucleocapsid protein of virulent mouse hepatitis virus is dependent on host hepatic nuclear factor-4_{α}. *J. Biol. Chem.* **278**, 15541–15549.
56. Gilch, S., Nunziante, M., Ertmer, A., Wopfner, F., Laszlo, L. & Schatzl, H. M. (2004). Recognition of lumenal prion protein aggregates by post-ER quality control mechanisms is mediated by the preoctarepeat region of PrP. *Traffic*, **5**, 300–313.